Canadian Conference - Pacific Conference on Earthquake Engineering 2023
Vancouver, British Columbia
June 25th – June 30th, 2023

NUMERICAL ANALYSIS OF TWO-STORY CLT BUILDING AND INFLUENCE OF ORTHOGONAL WALL CONNECTIONS

Tongchen Han[1*], Marjan Popovski[2], Thomas Tannert[3], Solomon Tesfamariam[4]

[1] PhD student, School of Engineering, The University of British Columbia, Okanagan Campus, 3333 University Way, Kelowna, BC, Canada
[2] Lead Scientist, Building Systems, FPInnovations, 2665 East Mall, Vancouver, BC, Canada
[3] Professor, School of Engineering, University of Northern British Columbia, 3333 University Way, Prince George BC, Canada
[4] Professor, School of Engineering, The University of British Columbia, Okanagan Campus, 3333 University Way, Kelowna, BC, Canada
[*]touch01@mail.ubc.ca (Corresponding Author)

ABSTRACT

Cross-laminated timber (CLT) is mass-timber product which is becoming popular in the North American construction market. CLT shear walls are an effective lateral load resistance system for high seismic activity or high wind loads. In this paper, the development of a numerical model of a two-story CLT shear wall building using user elements in the general purpose finite element software ABAQUS is presented. In-plane shear connections in CLT shear walls, e.g. angle brackets and hold-downs, are extensively studied and their impact on the shear wall performance is well understood. However, orthogonal connections between two perpendicular walls are often neglected, although these have been shown to significantly impact the shear wall behaviour. The numerical model presented herein accounts for different stiffness of orthogonal connections, ranging from rigid joints to zero-stiffness joints. The hysteretic behavior of a two-story CLT building including is evaluated and it is shown that its hysteretic behavior and the global response vary with the joints' stiffness.

Keywords: Cross-laminated timber (CLT), Finite element model, Orthogonal wall connections, Hysteretic behavior

INTRODUCTION

Background

In North America, Cross-laminated timber (CLT) shear wall structures are increasingly being used for residential buildings. Large-scale shake-table tests and numerical analyses of CLT buildings [1-4] proved their good seismic performances. Components in CLT shear wall building are connected by different types of connections; their mechanical properties influence the structural response. Angle brackets and hold-downs have been thoroughly investigated, concerning their in-plane hysteretic behaviors [5], out-of-plane hysteretic behaviors [6], or damage assessments [7] [8]. Angle brackets and hold-downs attached to the CLT panels with dowel-type fasteners usually showed 'pinching' behavior under hysteretic loading. Under in-plane or out-of-plane monotonic loading, the envelop curves of these connections were simplified to a tri-linear model. Some researchers also focused on the influence of wall-floor connections on the global response of CLT shear wall structures [9, 10]. The rocking stiffness and bending stiffness of CLT shear walls varied with changes in the stiffness and spacing of wall-floor connections. The coupling ratio of CLT shear walls was influenced by the strength of wall-floor connections.

The impact of orthogonal wall connections (OWC) on the mechanical properties of shear wall structures was also investigated [11]. The deflection of the shear walls decresed with increasing OWC stiffness. The location of the orthogonal wall also affected the strength of shear wall [12]. An orthogonal wall on compressive side did not influence the lateral performance of the shear wall, while an orthogonal wall on tensile side or center improved the lateral strength. Experimental tests for C-shaped CLT rocking walls also considered the influence of OWC [13], indicating that the strengthened OWC (mixed-angle screwed connections) could provide additional displacement and energy dissipation capacity. The above studies

on OWC were conducted on single/coupled shear walls under monotonic loading, while further research should focus on the global hysteretic response of CLT buildings.

Experimental test of two-story CLT shear wall building

Experimental tests of a two-story CLT shear wall building were conducted by Popovski and Gavric [14]. The building was 6.0 m in length (E-W direction), 4.8 m in width (N-S direction), and 4.8 m in height, as shown in Fig. 2. Both shear walls and floors were 94 mm in thickness with a density of 400 kg/m^3. The height of the story was 2.4 m. The first story consisted of two shear walls with openings on the west and east sides. For the shear wall on west side, the door opening was 2200 mm in length and 1900 mm in height. The opposite wall had a 900 mm × 1900 mm door opening and an additional window opening. Two partition walls with a width of 1600 mm were arranged in the first and second stories.

Hold-downs (HTT4) and angle brackets (BMF 90×48×3×116 mm) were placed at the bottom of the shear wall, connecting the shear wall and floor. Hold-downs were placed at the corner of the wall to reduce the uplift of the shear wall while angle brackets were placed at the middle section of the wall to resist the shear force. For the other connections in the building, e.g. connections between adjacent walls and connections between the wall and the upper floor, screws were used.

Experimental tests 3 and 4 were hysteretic loading tests in the E-W direction and N-S direction, respectively. There were two actuators in the experimental tests: the upper one was placed at the level of the second floor and the lower one was placed at the level of the first floor. The ISO load protocol [15] was adopted. Tests were conducted until the lateral displacement at the top of the building reached 1.75% of the total building height (84 mm). The loading rate was 2.54 mm/s.

The loading results are shown in Fig. 3 and Fig. 4. Wood failure and nail failure were observed along the loading direction. Yielding and withdrawal of nails in angle brackets and withdrawal of nails in hold-downs were detected. The shear slips of connections between adjacent walls and connections between the wall and the upper floor were very small.

Objective

Numerical models are recognized as an effective approach to investigating the structural response of complex systems. The phenomenological method [4] for the simulation of CLT structures is widely adopted for its computational simplicity. By simplifying the connections to nonlinear springs, macro-level numerical model for CLT structures can be developed. To investigate the influence of OWC strength on the global response of CLT buildings, the following tasks were undertaken:

- Development of a numerical model of CLT shear wall buildings with different OWC strengths.
- Model validation using experimental test results.
- Investigation of hysteretic properties, i.e., stiffness, bearing capacity, energy dissipation, and the ductility ratio of buildings with different OWC strengths.

NUMERICAL MODEL OF TWO-STORY CLT SHEAR WALL BUILDING

Model development

To simulate the hysteretic properties of hold-downs and angle brackets, a user element UELm [16] was developed in ABAQUS. The calibrated element was based on the UELo developed by Judd et al [17], and the hysteretic model is shown in Figure 1. The exponential curve developed by Folz and Filiatrault [18] was adopted as envelope curve, see Eq. (1):

$$\begin{aligned} F &= \operatorname{sgn}(Disp)\left(F_0 + K_1|Disp|\right)\left(1-e^{-K_2|Disp|/F_0}\right), |Disp| < |D_m| \\ F &= \operatorname{sgn}(Disp)\left(F_m + K_3\left(|Disp| - |D_m|\right)\right)\left(1-e^{-K_2|Disp|/F_0}\right), |D_f| \geq |Disp| \geq |D_m| \\ F &= 0, |D_f| < |Disp| \end{aligned} \tag{1}$$

Details of the symbols in Eq. (1) are shown in Figure 1. There were six loading paths in the hysteretic model: loading path 1 is the envelop curve; loading path 2 is the post-peak curve; loading path 3 is the unloading curve; loading path 4 is the pinching curve; loading path 5 is the reloading curve; and loading path 6 is the failure curve. K_3 is the secant stiffness between the maximum force point (D_m, F_m) and failure point (D_f, F_f). K_4 is the unloading stiffness. F_1 is the pinching force. When the loading amplitude is small, there is no pinching, as shown in the orange loop. When the loading amplitude becomes larger, pinching develops, as shown in the red loop. This hysteretic model is named 'Q-pinch' [19].

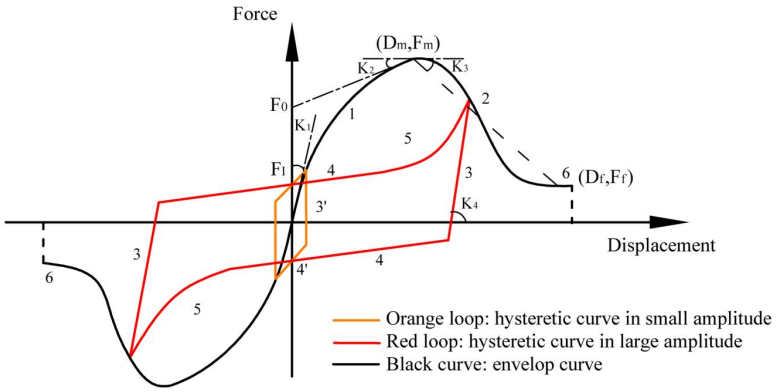

Figure 1. Hysteretic model of UELm.

The finite element model of the two-story CLT shear wall building as tested by Popovski and Gavric [14] was established in ABAQUS 2020, see Figure 2. The UELm was used for modelling the angle brackets and hold-downs. The locations of UELm were the same as the locations of angle brackets and hold-downs in tests 3 and 4. The property of CLT was simplified as isotropic, and the elasticity can be estimated through Blass–Fellmose method [20], as calculated in Eq. (2):

$$E = \frac{E_{90} n_p t + E_0 n_l t}{n} \tag{2}$$

where E_{90} is the elastic modulus of layers perpendicular to grain; E_0 is the elastic modulus of layers parallel to grain; n_p is the number of the layers perpendicular to grain; n_l is the number of the layers perpendicular to grain; t is the thickness of each layer; n is the number of layers. The steel elastic modulus, for the foundation was 20000 MPa, and its density was 8000 kg/m^3.

The CLT panel and steel beam foundation was modelled using 3-D solid shell element (S4R). In load module, the steel foundation was fixed, and the displacement-controlled load was applied using the experimental load data in tests 3 and 4. The dead load was applied on the roof of the model to simulate the stacked steel plates with magnitude of 0.47 kPa. The gravity load was also applied in the model. The general static step was set for the analysis of gravity load and dead load, as well as the cyclic loadings. In Figure 2, C1 and C2 represent the connections between shear wall and the upper floor. C3 represents the connections between parallel walls, and C4 represents the OWC. Considering the limited slip of screws in the tests, C1 to C4 were assumed to be rigid and were modelled with tie constraints.

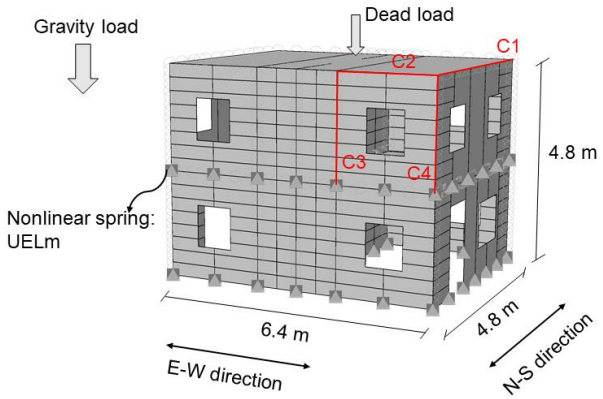

Figure 2. Finite element model of two-story CLT shear wall building.

Model validation

The test results of two-story CLT building were used for the validation of models. The comparison of hysteretic curves and energy dissipation curves in test 3 and test 4 are shown in Figure 3 and Figure 4, respectively. The hysteretic curves of models fit very well with the hysteretic curves of tests. The discrepancies in energy dissipation between model and test are 6% (test 3) and 2% (test 4). Eight parameters are listed in Table 1: F_u, D_u and $Drift_u$ are the ultimate force, ultimate displacement, and ultimate drift, respectively. The ultimate state was defined as the moment that the loading force of the structure dropped to 80% of the peak force. The model has a good agreement with experimental tests.

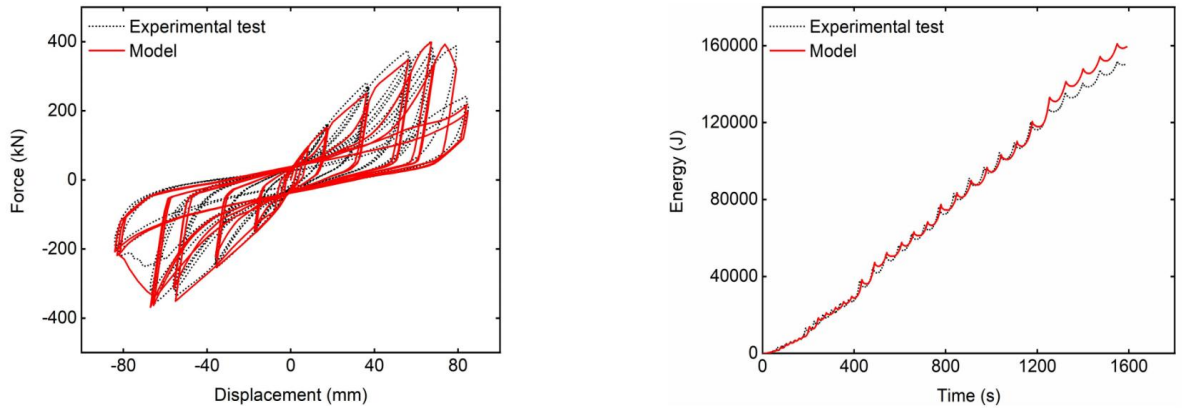

(a) *(b)*

Figure 3. Comparison of hysteretic curves and energy dissipation curves in test 3: (a) Comparison of hysteretic curves and (b) Comparison of energy dissipation curves.

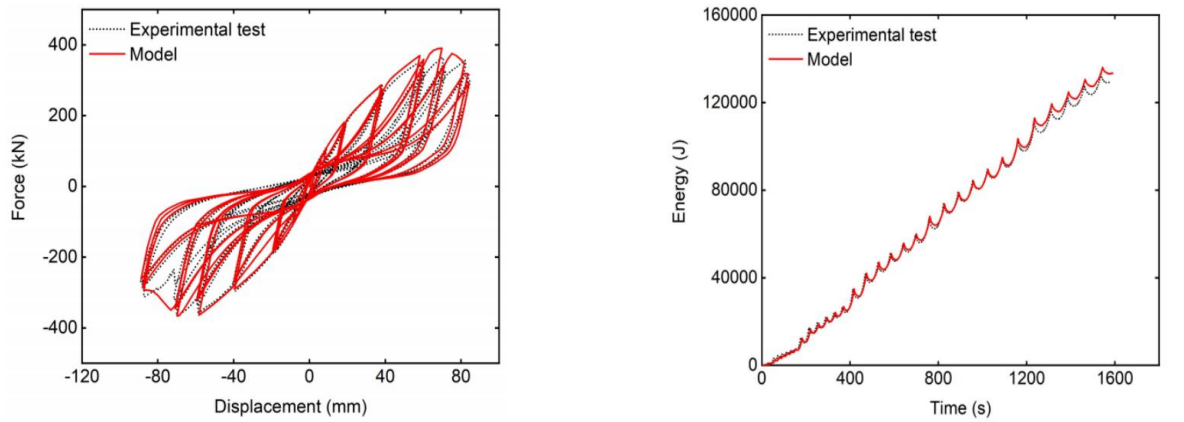

(a) *(b)*

Figure 4. Comparison of hysteretic curves and energy dissipation curves in test 4: (a) Comparison of hysteretic curves and (b) Comparison of energy dissipation curves.

Table 1. Comparison of test and model results.

Parameters	Test 3	Model	Error (%)	Test 4	Model	Error (%)
F_m (kN)	400.42	398.68	0.43	365.24	389.68	6.69
D_m (mm)	66.90	67.2	0.45	70.57	69.68	1.26
F_u (kN)	320.34	318.94	0.43	292.19	311.74	6.69
D_u (mm)	73.7	76.76	4.15	86.3	83.09	3.72
$Drift_u$ (%)	1.54	1.60	3.90	1.8	1.72	4.44
First story drift at D_u (%)	1.83	1.79	2.19	2.25	2.08	7.56
Second story drift at D_u (%)	1.25	1.41	12.80	1.34	1.36	1.49
Energy (J)	147.9	157.2	6.29	128.3	131.10	2.18

Influence of orthogonal wall connections

The effect of the strength of OWC (C4 in Figure 2) on the hysteretic behavior of shear wall building was studied through parametric analysis. The calibrated CLT building model in Section 2 was used for the numerical analysis. Five levels of OWC strengths were considered. In case of Level 1 (L1), the OWC was assumed to be rigid, therefore, model L1 was the originally developed model. Level 2 (L2) model included the angle uplift bracket's strength as OWC contribution, while Level 3 (L3) model included 1/2 of the angle bracket's strength. Level 4 (L4) had 1/4 of the angle bracket's strength, while the OWC for Level 5 (L5) model was set to zero. The uplift strength of the angle bracket in the building was 17 kN.

The hysteretic loading was conducted in the E-W direction and N-S direction using the same load protocol as the experimental test. Additionally, the monotonic loading was also conducted to get envelop curves of the building. The results are shown in Figure 5 and Figure 6. Some key results are listed in Table 2.

The strength of the building increases with the increase in the strength of OWC. For E-W direction loading, the maximum force F_m of L1 is 63% larger than the F_m of L5. For N-S direction loading, the F_m of L1 is 29% larger than the F_m of L5. Furthermore, the energy dissipation of the building increase with the increase in the strength of OWC. For E-W direction loading, the energy dissipation of L1 is 87% larger than the energy dissipation of L5. For N-S direction loading, the energy dissipation of L1 is 29% larger than the energy dissipation of L5.

The influence of OWC strength on the building is apparent according to the comparison between the L1 and L5. Except for the in-plane hold-downs and angle brackets, the hold-downs and angle brackets perpendicular to the loading direction (out-of-plane) also contribute to the total resistance. With increasing OWC strength, the participation level of out-of-plane hold-downs and angle brackets enhances, which affects the strength of the building [12]. This phenomenon is more significant in the E-W direction loading, according to the comparison between cases L1 and L5. For E-W direction loading, the number of in-plane hold-downs and angle brackets was 36, and the number of out-of-plane hold-downs and angle brackets was 46. On the contrary, the N-S direction had 46 in-plane hold-downs and angle brackets and 36 out-of-plane hold-downs and angle brackets. Therefore, the out-of-plane connections play more important roles in E-W direction loading than in N-S direction loading. The increase of OWC strength, which led to the activity of out-of-plane hold-downs and angle brackets, had a greater impact on E-W direction loading than on N-S direction loading.

The ductility ratio δ of the building can be determined through Eq. (3):

$$\delta = \frac{D_u}{D_y} \tag{3}$$

where D_u is the displacement at the ultimate force; D_y is the yielding displacement. To determine the yielding displacement, the yielding force and equivalent energy elastic-plastic (EEEP) curves need to be calculated. In the EEEP curve, the plastic portion is characterized by a horizontal line equal to the yielding force F_y. The F_y is calculated by Eq. (4) [21].

$$F_y = \left(D_u - \sqrt{D_u^2 - \frac{2A}{K_e}} \right) K_e \tag{4}$$

where A is the area under the envelop curve from zero to ultimate displacement D_u; K_e is the equivalent shear stiffness, which can be calculated as:

$$K_e = \frac{0.4F_m}{D_{40\%}} \tag{5}$$

where $D_{40\%}$ is the displacement at the 40% maximum force. Finally, the yielding displacement D_y is determined:

$$D_y = \frac{F_y}{K_e} \tag{6}$$

The EEEP curves of E-W direction loading and N-S direction loading are shown in Figure 5(b) and Figure 6(b). It can be seen that the equivalent shear stiffness K_e increases with the increase of OWC strength. And the stiffness degradation is more significant in E-W direction loading than in N-S direction loading.

The ductility ratios are also listed in Table 2. In experimental tests, the ductility ratios of E-W direction loading and N-S direction loading were 2.0 and 3.1, respectively. In model L1, the ductility ratios of E-W direction loading and N-S direction loading were 1.93 and 2.97, respectively. The model results were close to the experimental test results, which further validates the model developed in Section 2. For E-W direction loading and N-S direction loading, with the increase of OWC strength, the ductility ratios increase initially and then decrease, which indicates that moderate OWC strength can enhance the ductility of the building. Additionally, the building has greater ductility in N-S direction than in E-W direction in each case.

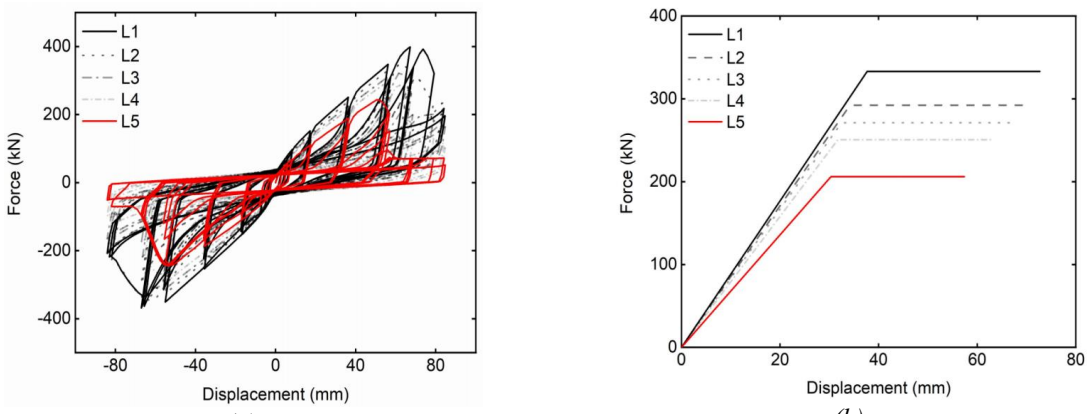

Figure 5. E-W direction loading results: (a) Hysteretic curves and (b)EEEP curves.

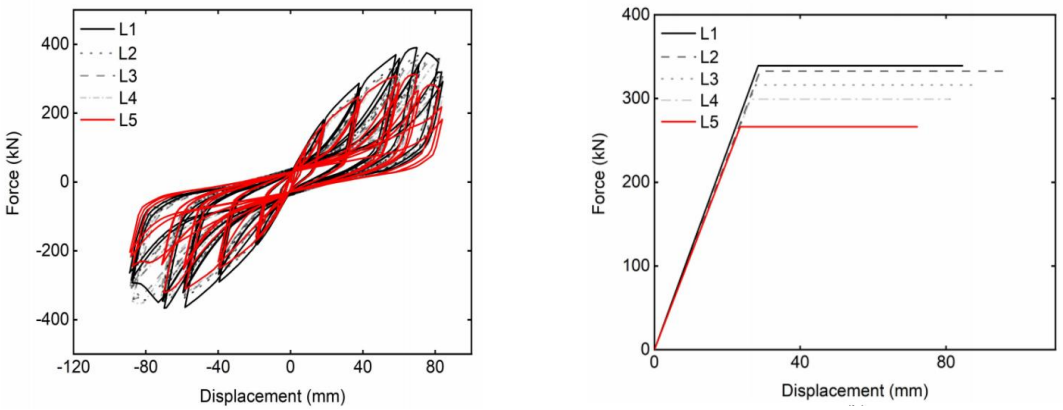

Figure 6. N-S direction loading results: (a) Hysteretic curves and (b) EEEP curves.

Table 2. Hysteretic properties analysis.

Direction	Case	F_m (kN)	D_m (mm)	Energy (kJ)	δ
E-W	L1	398	64.36	157	1.93
	L2	346	60.71	147	2.06
	L3	321	57.68	126	2.06
	L4	296	55.45	104	1.99
	L5	244	50.8	84	1.89
N-S	L1	399	68.16	133	2.97
	L2	384	75.51	131	3.36
	L3	366	72.64	129	3.16
	L4	346	69.32	120	3.08
	L5	310	63.82	103	3.06

CONCLUSIONS

In this study, a numerical model of CLT building was developed and validated against data from existing experimental tests. The impact of five levels of OWC strengths on the building performance were investigated. The model was subjected to reversible cyclic loading in the N-S direction and E-W direction of the building. The major conclusions of this study are:

- The numerical model of the CLT building exhibited similar global response to that observed during the experimental test. The maximum force, story drift, and energy dissipation of the model were close to the test with discrepancies of no more than 13%.
- With increasing OWC strength, the resistance provided by out-of-plane angle brackets and hold-downs increased, which led to the improvements of bearing capacity and energy dissipation capacity of the building. Compared with N-S

direction, E-W direction had more out-of-plane hold-downs and angle brackets, and this improvement was more significant.

- With increasing OWC strength, the ductility ratio of the building increased initially and then decreased. The building had higher ductility with OWC with moderate strength.

ACKNOWLEDGMENTS

This study was funded by Natural Sciences and Engineering Research Council of Canada under the Discovery Grant programs (RGPIN-2019-05584). Development of the design guideline in this study was supported through the BC Forestry Innovation Investment's (FII) Wood First Program.

REFERENCES

[1] Ceccotti, A., Sandhaas, C., Okabe, M., Yasumura, M., Minowa, C., and Kawai, N. (2013). SOFIE project-3D shaking table test on a seven-storey full-scale cross-laminated timber building. *Earthquake Engineering & Structural Dynamics*, 42(13), 2003-2021.

[2] Ceccotti, A. (2008). New technologies for construction of medium-rise buildings in seismic regions: the XLAM case. *Structural Engineering International*, 18(2), 156-165.

[3] Teweldebrhan, B. T., and Tesfamariam, S. (2022). Performance-based design of tall-coupled cross-laminated timber wall building. *Earthquake Engineering & Structural Dynamics*, 51(7), 1677-1696.

[4] Tesfamariam, S., Wakashima, Y., and Skandalos, K. (2021). Damped timber shear wall: Shake-table tests and analytical models. *Journal of Structural Engineering*, 147(6), 04021064.

[5] Shen, Y. L., Schneider, J., Tesfamariam, S., Stiemer, S. F., and Mu, Z. G. (2013). Hysteresis behavior of bracket connection in cross-laminated-timber shear walls. *Construction and Building Materials*, 48, 980-991.

[6] Rezvani, S., Zhou, L., and Ni, C. (2021). Experimental evaluation of angle bracket connections in CLT structures under in-and out-of-plane lateral loading. *Engineering Structures*, 244, 112787.

[7] Schneider, J., Shen, Y., Stiemer, S. F., and Tesfamariam, S. (2015). Assessment and comparison of experimental and numerical model studies of cross-laminated timber mechanical connections under cyclic loading. *Construction and Building Materials*, 77, 197-212.

[8] Krätzig, W. B., Meyer, I. F., and Meskouris, K. (1989). Damage evolution in reinforced concrete members under cyclic loading. *Structural safety and reliability,* (pp. 795-804).

[9] Tamagnone, G., Rinaldin, G., and Fragiacomo, M. (2020). Influence of the floor diaphragm on the rocking behavior of CLT walls. *Journal of Structural Engineering*, 146(3), 04020010.

[10] D'Arenzo, G., Schwendner, S., and Seim, W. (2021). The effect of the floor-to-wall interaction on the rocking stiffness of segmented CLT shear-walls. *Engineering Structures*, 249, 113219.

[11] Shahnewaz M, Popovski M, and Tannert T. Deflection of cross-laminated timber shear walls for platform-type construction. *Engineering structures*. 221, 111091.

[12] Ruggeri E, D'Arenzo G, Fossetti M, and Seim W. Investigating the effect of perpendicular walls on the lateral behaviour of Cross-Laminated Timber shear walls. *Structures.* Vol. 46, pp. 1679-1695.

[13] Brown, J. R., Li, M., Palermo, A., Pampanin, S., and Sarti, F. (2021). Experimental testing of a low-damage post-tensioned C-shaped CLT core-wall. *Journal of Structural Engineering*, 147(3), 04020357.

[14] Popovski, M., and Gavric, I. (2016). Performance of a 2-story CLT house subjected to lateral loads. *Journal of Structural Engineering*, 142(4), E4015006.

[15] American Society for Testing and Materials - ASTM (2011). *ASTM E2126: Standard test methods for cyclic (reversed) load test for shear resistance of vertical elements of the lateral force resisting systems for buildings.*

[16] Han T. and Tesfamariam S. (2023) Numerical Analysis of CLT Shear Walls Using High-fidelity Model: Connection to Building System. *Journal of Building Engineering* (Accepted).

[17] Judd, J. P., and Fonseca, F. S. (2005). Analytical model for sheathing-to-framing connections in wood shear walls and diaphragms. *Journal of Structural Engineering,* 131(2), 345-352.

[18] Folz, B., and Filiatrault, A. (2001). Cyclic analysis of wood shear walls. *Journal of Structural Engineering,* 127(4), 433-441.

[19] Judd, J. P. (2005). *Analytical modeling of wood-frame shear walls and diaphragms*. Brigham Young University.

[20] Blass, H. J., and Fellmoser, P. (2004). Design of solid wood panels with cross layers. In *8th world conference on timber engineering* (Vol. 14, No. 17.6, p. 2004).

[21] Schneider, J., Karacabeyli, E., Popovski, M., Stiemer, S. F., and Tesfamariam, S. (2014). Damage assessment of connections used in cross-laminated timber subject to cyclic loads. *Journal of Performance of Constructed Facilities*, 28(6), A4014008.